J|A|C|S
ARTICLES
Published on Web 07/20/2002

On the Physical Origin of Blue-Shifted Hydrogen Bonds

Xiaosong Li,[†] Lei Liu,[‡] and H. Bernhard Schlegel*,[†]

Contribution from the Department of Chemistry, Wayne State University, Detroit, Michigan 48202, and Department of Chemistry, Columbia University, New York, New York 10027

Received February 11, 2002. Revised Manuscript Received May 20, 2002

Abstract: For blue-shifted hydrogen-bonded systems, the hydrogen stretching frequency increases rather than decreases on complexation. In computations at various levels of theory, the blue-shift in the archetypical system, $F_3C-H\cdots FH$, is reproduced at the Hartree−Fock level, indicating that electron correlation is not the primary cause. Calculations also demonstrate that a blue-shift does not require either a carbon center or the absence of a lone pair on the proton donor, because $F_3Si-H\cdots OH_2$, $F_2NH\cdots FH$, $F_2PH\cdots NH_3$, and $F_2PH\cdots OH_2$ have substantial blue-shifts. Orbital interactions are shown to lengthen the X−H bond and lower its vibrational frequency, and thus cannot be the source of the blue-shift. In the $F_3CH\cdots FH$ system, the charge redistribution in F_3CH can be reproduced very well by replacing the FH with a simple dipole, which suggests that the interactions are predominantly electrostatic. When modeled with a point charge for the proton acceptor, attractive electrostatic interactions elongate the F_3C-H, while repulsive interactions shorten it. At the equilibrium geometry of a hydrogen-bonded complex, the electrostatic attraction between the dipole moments of the proton donor and proton acceptor must be balanced by the Pauli repulsion between the two fragments. In the absence of orbital interactions that cause bond elongation, this repulsive interaction leads to compression of the X−H bond and a blue-shift in its vibrational frequency.

Introduction

The hydrogen bond, which plays a crucial role in chemistry and biology, is normally characterized as a relatively weak interaction involving an electronegative proton donor X, a hydrogen, and an electronegative proton acceptor Y.[1−5] The interaction is believed to be predominantly electrostatic in nature, although charge-transfer interactions are also important.[6−9] According to the classical electrostatic model of hydrogen bonding, the electron density of Y exerts an attractive force on the proton, and the approach of Y should always lengthen the X−H bond.[10] On the other hand, if significant charge transfer occurs from the proton acceptor Y to the proton donor, in particular to the X−H σ^* antibonding orbital, the X−H bond should also be weakened upon the hydrogen bond formation and concomitantly elongated.[11] This elongation of the X−H bond results in a decrease in the X−H stretching vibration frequency, and such a red-shift has been used in many experimental studies as evidence of hydrogen bond formation.[12,13] The extent of the red-shift has been correlated with the strength of the hydrogen bond,[14] the proton donor−acceptor distance,[15,16] and the ionization potential of the proton acceptor.[17]

In a few cases, however, experiments find that the X−H stretching vibration is shifted toward higher frequency (blue-shift) in an X−H···Y hydrogen-bonded system,[18−31] where X is CF_3 and CCl_3, and Y is triformylmethane, benzene, ethylene oxide, and dimethyl ether. A number of theoretical studies have also demonstrated that blue-shifted hydrogen bonds can be obtained at various levels of calculation.[29−44] Clearly, this challenges the generally held explanations of hydrogen bonding

* To whom correspondence should be addressed. E-mail: hbs@chem.wayne.edu.
[†] Wayne State University.
[‡] Columbia University.

(1) Huggins, M. L. *Science* **1922**, *55*, 459.
(2) Pauling, L. *J. Am. Chem. Soc.* **1931**, *53*, 1367.
(3) Scheiner, S. *Hydrogen Bonding*; Oxford University Press: New York, 1997.
(4) Jeffrey, G. A. *An Introduction to Hydrogen Bond*; Oxford University Press: New York, 1997.
(5) Desiraju, G.; Steiner, T. *The Weak Hydrogen Bond*; Oxford University Press: New York, 1999.
(6) Kollman, P. A.; Allen, L. C. *Chem. Rev.* **1972**, *72*, 283.
(7) Gordon, M. S.; Jensen, J. H. *Acc. Chem. Res.* **1996**, *29*, 536.
(8) Morokuma, K. *Acc. Chem. Res.* **1977**, *10*, 294.
(9) Liu, S.; Dykstra, C. E. *J. Phys. Chem.* **1986**, *90*, 3097.
(10) Bader, R. F. W. *Can. J. Chem.* **1964**, *42*, 1822.
(11) Ratajczak, H. *J. Phys. Chem.* **1972**, *76*, 3000.
(12) Tichy, M. *Adv. Org. Chem.* **1965**, *5*, 115.
(13) Sandorfy, C. *Top. Curr. Chem.* **1984**, *120*, 41.
(14) Badger, R. M.; Bauer, S. H. *J. Chem. Phys.* **1937**, *5*, 839.
(15) Nakamoto, K.; Margolis, M.; Rundel, R. E. *J. Am. Chem. Soc.* **1955**, *77*, 6480.
(16) Ojamae, L.; Hermansson, K. *J. Chem. Phys.* **1992**, *96*, 9035.
(17) Szczepaniak, K.; Tramer, A. *J. Phys. Chem.* **1967**, *71*, 9.
(18) Pinchas, S. *Anal. Chem.* **1957**, *29*, 334.
(19) Pinchas, S. *J. Phys. Chem.* **1963**, *67*, 1862.
(20) Satonaka, H.; Abe, K.; Hirota, M. *Bull. Chem. Soc. Jpn.* **1987**, *60*, 953.
(21) Budesinsky, M.; Fiedler, P.; Arnold, Z. *Synthesis* **1989**, 858.
(22) Boldeskul, I. E.; Tsymbal, I. F.; Ryltsev, E. V.; Latajka, Z.; Barnes, A. J. *J. Mol. Struct.* **1997**, *437*, 167.
(23) Caminati, W.; Melandri, S.; Moreschini, P.; Favero, P. G. *Angew. Chem., Int. Ed.* **1999**, *38*, 2924.
(24) Mizuno, K.; Imafuji, S.; Ochi, T.; Ohta, T.; Maeda, S. *J. Phys. Chem. B* **2000**, *104*, 11001.
(25) Goutev, N.; Matsuura, H. *J. Phys. Chem. A* **2001**, *105*, 4741.
(26) Reimann, B.; Buchhold, K.; Vaupel, S.; Brutschy, B. *Z. Phys. Chem.* **2001**, *215*, 777.
(27) Afonin, A. V.; Andriyankov, M. A. *Zh. Org. Khim.* **1988**, *24*, 1034.
(28) Keshavarz-K, M.; Cox, S. D.; Angus, R. O.; Wudl, F. *Synthesis* **1988**, 641.
(29) Cubero, E.; Orozco, M.; Hobza, P.; Luque, F. J. *J. Phys. Chem. A* **1999**, *103*, 6394.
(30) van der Veken, B. J.; Herrebout, W. A.; Szostak, R.; Shchepkin, D. N.; Havlas, Z.; Hobza, P. *J. Am. Chem. Soc.* **2001**, *123*, 12290.
(31) Hobza, P.; Havlas, Z. *Chem. Rev.* **2000**, *100*, 4253.

and the standard experimental methods of detecting hydrogen bonds, because the qualitative theoretical models mentioned above only allow for red-shifts.

Hobza and co-workers[29−34] have proposed that blue-shifted hydrogen bonding can be explained by charge transfer from the proton acceptor Y to remote (presumably highly electronegative) atoms in X (e.g., F in CF_3) instead of the X−H σ^* antibonding orbitals, followed by a structural reorganization of the proton donor framework resulting in contraction of the X−H bond. Thus, the red-shifted and blue-shifted hydrogen bonds were deemed to have different origins. In sharp contrast to this theory, S. Scheiner and co-workers[42,44] found that the C−H···O interaction in CF_nH_{3-n}−H···O was very much like a conventional O−H···O H-bond in terms of geometric behavior, charge redistribution, and energy component analysis. They concluded that the blue-shifted C−H bond in C−H···O was a true H-bond but did not provide a detailed description of the origin of blue-shift. Dykstra and co-workers[9,45−47] have developed a theory of vibrational frequency shifts in hydrogen bonding based on monomer properties such as electrical moments and polarizabilities. For red-shifted hydrogen bonds, electrostatic interactions account for a major portion of the shift, with polarizabilities increasing the shift further.

All of the blue-shifted hydrogen bonds that have been studied so far are exclusively C−H···Y systems; it is not yet known whether blue-shifted hydrogen bonds can be observed when the central atom of the proton donor is not carbon. Moreover, it appears that all of the blue-shifted hydrogen bonds examined have highly electronegative atoms (e.g., F, Cl) in the proton donor; it is unclear whether this must always be true. Thus, several fundamental and interesting questions about the blue-shifted hydrogen bonding remain unanswered. One goal of our study is to find cases of blue-shifted hydrogen bonds where the central atom of the proton donor is not carbon and where the central atom has a lone pair. Armed with more examples, our next goal is to compare various aspects of the blue-shifted hydrogen bonds in a systematic manner, to test a number of explanations of the possible physical origins of the blue-shift. Hopefully, the resulting explanation will provide a unified, first principles description for both blue-shifted and red-shifted hydrogen bonds.

Method

All of the calculations were performed with the development version of the Gaussian series of programs.[48] To explore the dependence of the blue-shift on the methods and basis sets, the F_3C−H···FH hydrogen-bonded complex was studied by semiempirical (AM1, PM3), Hartree−Fock (HF), B3LYP, and post-SCF [MP2(FC), MP2(Full)] theories with a minimal basis set (STO-3G), and split valence basis sets with and without polarization and diffusion functions [3-21G, 6-31G, 6-311+G(d,p), 6-311++G(d,p)]. At each level of theory, the geometry was fully optimized without symmetry constraints. This established that MP2(FC)/6-311+G(d,p) adequately described blue-shifted hydrogen bonds, and this level of theory was used for all subsequent calculations.

All of the hydrogen-bonded systems were found to be actual minima as confirmed by a frequency calculation at the MP2(FC)/6-311+G(d,p) level of theory. Because no symmetries were enforced in optimizations, except in the F_3C−H···NH_3 complex, the ∠XHY angles in the equilibrium geometries were found to be nonlinear. Mulliken charge distributions[49] and natural bond orbital population analysis[50−53] were also obtained for both monomers and hydrogen-bonded systems.

Hydrogen bond energies were corrected for basis set superposition error (BSSE). This was estimated for each hydrogen-bonded system with the full counterpoise method[54] using the expression

$$\delta_{XY}^{BSSE} = E_{XY}^{X}(X) - E_{XY}^{XY}(X) + E_{XY}^{Y}(Y) - E_{XY}^{XY}(Y) \qquad (1)$$

where $E_A^B(C)$ represents the energy of system C at geometry A with basis set B.

Electron density difference maps were generated by applying the following method:

$$\Delta D_{complex} = D(F_3CH\cdots FH) - D(F_3CH) - D(FH)$$

$$\Delta D_{dipole} = D(F_3CH\cdots dipole) - D(F_3CH)$$

where D(S) represents the electron density of system S at geometry F_3C−H···FH with a basis set of F_3C−H···FH.

Results and Discussion

A. Dependence of the Blue-Shift on the Level of Theory. To determine the effect of the theoretical methods and basis sets on the calculated bond lengths, we performed geometry optimizations on the F_3C−H···FH complex with semiempirical, HF, DFT, and MP2 theories with various basis sets. The results are summarized in Table 1. Semiempirical methods such as AM1 and PM3 fail to predict blue-shifts. In fact, they predict a bond elongation, which is contrary to the results of higher level calculations. This could have been anticipated, because weak interactions such as van der Waals interaction and hydrogen bonding are poorly modeled by these methods; either the interaction energy is too small, or the minimum energy geometry is wrong.[55] This is yet another reason for disfavoring the use of AM1 or PM3 methods in modeling hydrogen bonding.

(32) Hobza, P.; Spirko, V.; Havlas, Z.; Buchhold, K.; Reimann, B.; Barth, H. D.; Brutschy, B. *Chem. Phys. Lett.* **1999**, *299*, 180.
(33) Hobza, P.; Spirko, V.; Selzle, H. L.; Schlag, E. W. *J. Phys. Chem. A* **1998**, *102*, 2501.
(34) Reimann, B.; Buchhold, K.; Vaupel, S.; Brutschy, B.; Havlas, Z.; Spirko, V.; Hobza, P. *J. Phys. Chem. A* **2001**, *105*, 5560.
(35) Hobza, P.; Havlas, Z. *Chem. Phys. Lett.* **1999**, *303*, 447.
(36) Hobza, P.; Sponer, J.; Cubero, E.; Orozco, M.; Luque, F. J. *J. Phys. Chem. B* **2000**, *104*, 6286.
(37) Cubero, E.; Orozco, M.; Luque, F. J. *Chem. Phys. Lett.* **1999**, *310*, 445.
(38) Muchall, H. M. *J. Phys. Chem. A* **2001**, *105*, 632.
(39) Masunov, A.; Dannenberg, J. J.; Contreras, R. H. *J. Phys. Chem. A* **2001**, *105*, 4737.
(40) Hocquet, A. *Phys. Chem. Chem. Phys.* **2001**, *3*, 3192.
(41) Kryachko, E. S.; Zeegers-Huyskens, T. *J. Phys. Chem. A* **2001**, *105*, 7118.
(42) Gu, Y. L.; Kar, T.; Scheiner, S. *J. Am. Chem. Soc.* **1999**, *121*, 9411.
(43) Scheiner, S.; Kar, T.; Gu, Y. L. *J. Biol. Chem.* **2001**, *276*, 9832.
(44) Scheiner, S.; Kar, T. *J. Phys. Chem. A* **2002**, *106*, 1784.
(45) Liu, S. Y.; Dykstra, C. E.; Malik, D. J. *Chem. Phys. Lett.* **1986**, *130*, 403.
(46) Liu, S. Y.; Dykstra, C. E. *Chem. Phys. Lett.* **1987**, *136*, 22.
(47) Parish, C. A.; Dykstra, C. E. *J. Phys. Chem.* **1993**, *97*, 9374.
(48) Frisch, M. J.; Trucks, G. W.; Schlegel, H. B.; Scuseria, G. E.; Robb, M. A.; Cheeseman, J. R.; Zakrzewski, V. G.; Montgomery, J. A.; Stratmann, R. E.; Burant, J. C.; Dapprich, S.; Millam, J. M.; Daniels, A. D.; Kudin, K. N.; Strain, M. C.; Farkas, O.; Tomasi, J.; Barone, V.; Cossi, M.; Cammi, R.; Mennucci, B.; Pomelli, C.; Adamo, C.; Clifford, S.; Ochterski, J.; Petersson, G. A.; Ayala, P. Y.; Cui, Q.; Morokuma, K.; Malick, D. K.; Rabuck, A. D.; Raghavachari, K.; Foresman, J. B.; Cioslowski, J.; Ortiz, J. V.; Stefanov, B. B.; Liu, G.; Liashenko, A.; Piskorz, P.; Komaromi, I.; Gomperts, R.; Martin, R. L.; Fox, D. J.; Keith, T.; Al-Laham, M. A.; Peng, C. Y.; Nanayakkara, A.; Gonzalez, C.; Challacombe, M.; Gill, P. M. W.; Johnson, B. G.; Chen, W.; Wong, M. W.; Andres, J. L.; Head-Gordon, M.; Replogle, E. S.; Pople, J. A. *Gaussian 99*; Gaussian, Inc.: Pittsburgh, PA, 1999.
(49) Mulliken, R. S. *J. Chem. Phys.* **1955**, *23*, 2343.
(50) Foster, J. P.; Weinhold, F. *J. Am. Chem. Soc.* **1980**, *102*, 7211.
(51) Carpenter, J. E.; Weinhold, F. *THEOCHEM J. Mol. Struct.* **1988**, *46*, 41.
(52) Reed, A. E.; Weinhold, F. *J. Chem. Phys.* **1983**, *78*, 4066.
(53) Reed, A. E.; Weinstock, R. B.; Weinhold, F. *J. Chem. Phys.* **1985**, *83*, 735.
(54) Boys, S. F.; Bernardi, F. **1970**, *19*, 553.
(55) Jensen, F. *Introduction to Computational Chemistry*; John Wiley & Sons: New York, 1999.

Table 1. Dependence of CH Bond Length (Å) and Interaction Energy (kcal/mol) on the Methods and Basis Sets for the $F_3C-H\cdots FH$ System

method	*R*(CH) (monomer)	*R*(CH) (complex)	ΔE
AM1	1.1301	1.1316	−2.7
PM3	1.1099	1.1120	−1.6
HF/STO-3G	1.119	1.1206	−1.8
HF/3-21G	1.0659	1.0615	−7.6
HF/6-31G	1.0673	1.0652	−5.6
HF/6-311+G(d,p)	1.0766	1.0750	−2.5
HF/6-311++G(d,p)	1.0766	1.0750	−2.5
B3LYP/6-311+G(d,p)	1.0899	1.0880	−2.3
MP2(FC)/6-311+G(d,p)	1.0877	1.0852	−2.5
MP2(Full)/6-311+G(d,p)	1.0874	1.0847	−2.6

Table 2. H-Bonded Complex Geometries[a]

H-bonded system	H-donor monomer	complex with H-acceptor NH_3	SH_2	OH_2	ClH	FH
		$F_3C-H\cdots YH_n$				
∠C−H···Y		179.7	177.9	176.2	119.0	172.9
Y···H		2.2937	2.8290	2.1970	3.0295	2.2719
C−H	1.0878	1.0875	1.0862	1.0855	1.0868	1.0852
freq (C−H)	3222.3	3221.5	**3244.7**	**3260.2**	**3238.4**	**3268.1**
		$F_3Si-H\cdots YH_n$				
∠Si−H···Y		179.8	83.7	78.3		
Y···H		2.6992	3.5503	2.6776		
Si−H	1.4490	1.4480	1.4465	1.4444		
freq (Si−H)	2455.4	**2457.0**	**2469.0**	**2477.6**		
		$F_2N-H\cdots YH_n$				
∠N−H···Y		171.4	146.4	169.6	135.9	136.1
Y···H		1.9298	2.5364	2.5622	2.6584	2.1649
N−H	1.0261	1.0374	1.0294	1.0288	1.0270	1.0264
freq (N−H)	3443.4	3251.2	3392.1	3413.3	3439.5	**3456.8**
		$F_2P-H\cdots YH_n$				
∠P−H···Y		108.9	106.5	105.1		
Y···H		2.7199	3.3731	2.8081		
P−H	1.4135	1.4079	1.4112	1.4094		
freq (P−H)	2472.2	**2514.9**	**2490.7**	**2505.3**		
		$FO-H\cdots YH_n$				
∠O−H···Y		174.4	165.2	176.0	148.3	147.1
Y···H		1.7834	2.3731	1.7926	2.5058	1.9925
O−H	0.9684	0.9920	0.9754	0.9785	0.9710	0.9714
freq (O−H)	3811.0	3337.1	3664.0	3616.2	3764.4	3766.3
		$FS-H\cdots YH_n$				
∠S−H···Y		145.0	132.1	177.3		
Y···H		2.1405	2.8706	2.0894		
S−H	1.3365	1.3451	1.3379	1.3394		
freq (S−H)	2796.7	2680.7	2781.9	2761.8		

[a] Bond lengths in Å; frequencies in cm^{-1}; calculated at MP2(FC)/6-311+G(d,p).

On the other hand, except for HF/STO-3G, all of the Hartree−Fock and post-SCF methods (MP2 and DFT) with various basis sets predict that the C−H bond is shortened upon hydrogen bond formation. Although the detailed value of the prediction varies from one method to the other, it is apparent that the C−H contraction in the $F_3C-H\cdots FH$ system does not originate mainly from electron correlation or from the use of diffuse or polarization basis functions. The blue-shift is a phenomenon whose physical origin lies in interactions that can be sufficiently described by Hartree−Fock molecular orbital theory with even modest basis sets. This contradicts the explanation that the blue-shift is due to dispersion interactions,[35] because Hartree−Fock theory does not include dispersion interactions. Nevertheless, to get accurate values for the geometry and the interaction energy, it is clear that correlated methods with larger basis functions should be used. We choose MP2(FC)/6-311+G(d,p) in our further study.

Table 3. Interaction Energy (kcal/mol) Calculated at MP2(FC)/6-311+G(d,p)

H-bonded systems	complex with H-acceptor[a] NH_3	SH_2	OH_2	HCl	HF
	$F_3C-H\cdots YH_n$				
ΔE	−5.3	−2.7	−4.6	−2.5	−2.6
$\Delta E + \delta$BSSE	−3.9	−1.2	−3.3	−1.1	−1.9
	$F_3Si-H\cdots YH_n$				
ΔE	−2.3	−3.1	−6.2		
$\Delta E + \delta$BSSE	−1.4	−1.2	−3.6		
	$F_2N-H\cdots YH_n$				
ΔE	−9.9	−4.7	−7.7	−3.4	−4.3
$\Delta E + \delta$BSSE	−7.9	−2.7	−5.8	−1.7	−3.2
	$F_2P-H\cdots YH_n$				
ΔE	−3.5	−2.8	−3.6		
$\Delta E + \delta$BSSE	−2.0	−1.0	−1.9		
	$FO-H\cdots YH_n$				
ΔE	−12.0	−5.1	−9.1	−3.4	−4.8
$\Delta E + \delta$BSSE	−9.8	−3.4	−6.9	−1.9	−3.7
	$FS-H\cdots YH_n$				
ΔE	−6.1	−3.3	−4.9		
$\Delta E + \delta$BSSE	−4.5	−1.8	−3.4		

[a] Proton affinities for NH_3, H_2S, H_2O, HCl, and HF are 213.5, 146.4, 170.7, 79.4, and 102.8 kcal/mol, respectively.

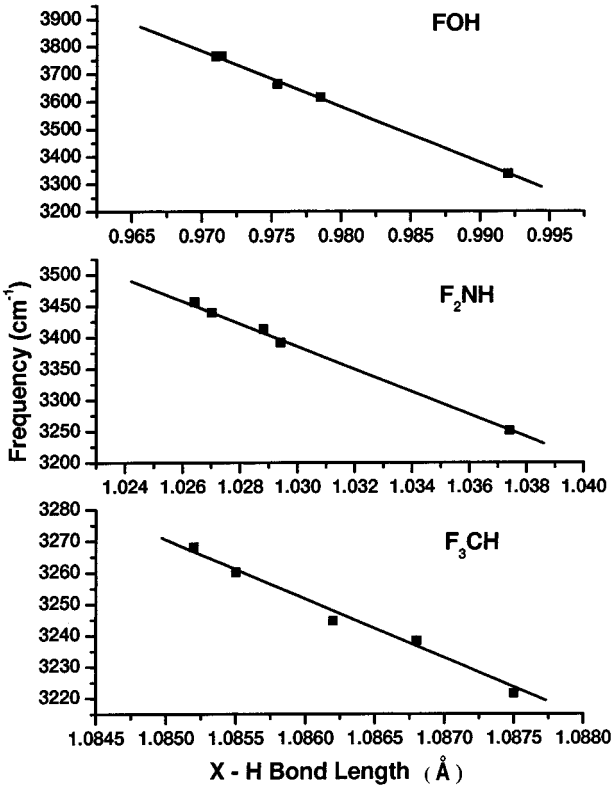

Figure 1. Relationship between C−H frequencies and C−H bond length (see Table 2).

B. Do Blue-Shifts Occur Only in Carbon-Centered Systems? Table 2 shows the geometries and harmonic vibrational frequencies without BSSE corrections for the proton donors and hydrogen-bonded complexes considered in the present study, calculated at MP2(FC)/6-311+G(d,p) level. Anharmonicity and BSSE correction may cause differences of 10−20%.[56,57] The

Table 4. Substituent Effect in $F_3C-H\cdots NR_nH_{3-n}$[a]

proton acceptor	monomer proton affinity	H-bonded complex ∠C–H···Y	H···Y	R(C–H)[b]	ΔE
NH_3	213.5	179.7	2.2937	1.0875	−5.3
NH_2F	190.6	173.3	2.3629	1.0854	−4.0
NHF_2	166.3	113.8	2.7266	1.0865	−2.9
NF_3	139.7	179.6	2.6600	1.0868	−1.0
NH_2Cl	200.5	177.4	2.2951	1.0868	−4.7
$NHCl_2$	189.9	178.1	2.2687	1.0864	−4.6
NCl_3	181.8	179.6	2.2406	1.0867	−4.5
NH_2CH_3	224.1	162.8	2.2556	1.0884	−5.4
$NH(CH_3)_2$	231.2	154.5	2.2446	1.0890	−5.7
$N(CH_3)_3$	235.6	177.6	2.2002	1.0904	−5.8

[a] Bond lengths in Å; bond angle in deg; proton affinity and ΔE without BSSE in kcal/mol; calculated at MP2(FC)/6-311+G(d,p). [b] R(C−H) = 1.0878 in F_3CH monomer.

interaction energies, with BSSE corrections and zero point vibration energies, are listed in Table 3.

The results show that blue-shifted hydrogen bonds are not confined to C−H···Y systems; Si−H···Y, N−H···Y, and P−H···Y complexes can exhibit such a behavior as well. Therefore, the presence of a carbon or the absence of a lone pair of electrons on the central atom of the proton donor, which are also possible explanations for the X−H contraction in X−H···Y interactions, is not the true physical origin of the blue-shift. Likewise, as all of the proton acceptors, from NH_3 to HCl, can cause blue-shifted as well as red-shifted hydrogen bonds, it is not a particular proton acceptor that causes the blue-shift.

A plot of the X−H vibrational frequencies versus the X−H bond lengths gives straight lines (Figure 1). The correlation coefficients range from 0.9900 to 0.9991, showing that these relations are excellent. Therefore, blue-shift means X−H contraction, and vice versa.

According to Table 3, the calculated interaction energy between F_3CH and Y decreases in the order H_3N > H_2O > H_2S > HF > HCl. This order is reasonable because the gas-phase basicity of the proton acceptors is in the same order, and the interaction strengths of other X−H···Y complexes approximately obey the order, as well. The only exceptions are $F_3Si-H\cdots OH_2$ and $F_3Si-H\cdots SH_2$, where, in addition to Si−H···YH hydrogen bonding, the Y−H···F−Si interaction is also involved, as indicated by the ∠X−H···Y angle (Table 2). Nevertheless, the extent of blue-shift or X−H contraction does not increase or decrease in the above order. It is the proton acceptors of intermediate basicity that cause the most significant blue-shift or X−H contraction. For example, HF causes the largest blue-shift when F_3CH is the proton donor. On the other hand, both more basic and less basic proton acceptors cause significant smaller blue-shifts or even cause a red-shift.

The hydrogen-bonded systems considered here are not associated with as large interaction energies as H_2O-H_2O or H_2O−HF. However, most of them can be designated as hydrogen bonds, as they display several of the key features of hydrogen bonds,[7,31,42,44] such as directionality in bonding and characteristic changes in the electron density distribution.

C. Blue-Shifts and Substituents on the Proton Acceptor. As described above, for a given proton donor, the blue-shift is the most significant for proton acceptors with intermediate basicity when the central atom of the acceptor is varied. It is also of interest to know if the same behavior can be observed when the proton acceptors have the same central atom but substituents are varied. The interaction energies and structural parameters for $F_3C-H\cdots NR_nH_{3-n}$ are summarized in Table 4. The results in Figure 2 show that the interaction energy decreases $N(CH_3)_3$ > $NH(CH_3)_2$ > NH_2CH_3 > NH_3 > NH_2Cl > $NHCl_2$ > NCl_3 > NH_2F > NHF_2 > NF_3, in the same order as the gas-phase basicities. However, the blue-shift is largest for $F_3C-H\cdots NH_2F$. Again, proton acceptors with too high or too low basicity appear to disfavor blue-shifts. Any theory of the blue-shift hydrogen bonds must be able to explain such behavior.

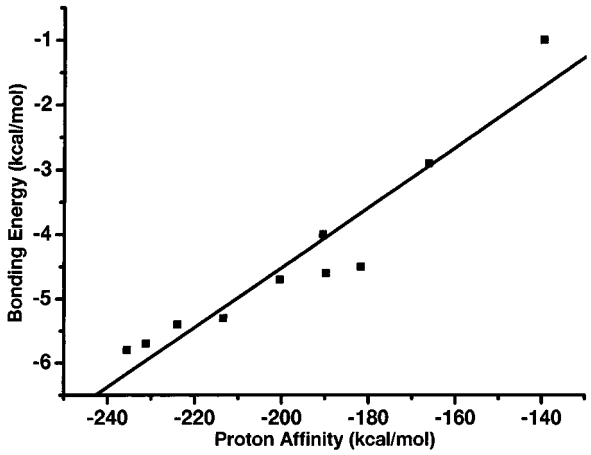

Figure 2. Relationship between hydrogen bond energy and proton affinity of hydrogen acceptor in $F_3C-H\cdots NH_{3-n}R_n$ (see Table 4).

Table 5. Natural Population Analysis for H-Bonded Complex[a]

systems	F	X	H	Y	H[b]	NCT[c]
F_3C-H	−0.3958	1.0825	0.1050			
$F_3C-H\cdots NH_3$	−0.4058	1.0503	0.1582	−1.0490	0.3526	−0.0089
$F_3C-H\cdots SH_2$	−0.3995	1.0655	0.1273	−0.2380	0.1219	−0.0057
$F_3C-H\cdots OH_2$	−0.4037	1.0584	0.1483	−0.9384	0.4714	−0.0044
$F_3C-H\cdots ClH$	−0.3983	1.0765	0.1177	−0.2618	0.2625	−0.0007
$F_3C-H\cdots FH$	−0.4001	1.0692	0.1296	−0.5667	0.5682	−0.0015
F_2N-H	−0.2882	0.2515	0.3250			
$F_2N-H\cdots NH_3$	−0.3110	0.2051	0.3876	−1.0576	0.3623	−0.0293
$F_2N-H\cdots SH_2$	−0.2988	0.2317	0.3497	−0.2412	0.1287	−0.0162
$F_2N-H\cdots OH_2$	−0.3054	0.2234	0.3748	−0.9466	0.4796	−0.0126
$F_2N-H\cdots ClH$	−0.2951	0.2464	0.3403	−0.2641	0.2675	−0.0035
$F_2N-H\cdots FH$	−0.2992	0.2460	0.3501	−0.5711	0.5735	−0.0023
FO−H	−0.1934	−0.2748	0.4682			
$FO-H\cdots NH_3$	−0.2345	−0.3223	0.5126	−1.0540	0.3661	−0.0442
$FO-H\cdots SH_2$	−0.2130	−0.2972	0.4863	−0.2347	0.1239	−0.0239
$FO-H\cdots OH_2$	−0.2234	−0.3038	0.5078	−0.9463	0.4829	−0.0194
$FO-H\cdots ClH$	−0.2126	−0.2745	0.4811	−0.2632	0.2692	−0.0060
$FO-H\cdots FH$	−0.2209	−0.2755	0.4911	−0.5713	0.5765	−0.0053

[a] NPA for Y in monomers of hydrogen acceptor, NH_3, H_2S, H_2O, HCl, HF are −1.0298, −0.2233, −0.9173, −0.2477, −0.5574, respectively. [b] H on Y. [c] Net charge transferred from hydrogen donor.

D. Is Charge Transfer the Origin of the Blue-Shift? Among the proposed explanations for blue-shifted hydrogen bonds, charge transfer appears as the first choice. However, charge transfer is not a physical observable and is often difficult to quantify computationally in a manner that is not sensitive to the level of theory. Natural bond orbital population analyses for the hydrogen-bonded systems are listed in Table 5; Mulliken charges show the same trends. For the systems with substantial red-shifts (F_2N-H and FO−H with NH_3, OH_2, and SH_2), the net charge transfer is significant. However, for the blue-shifted

(56) Silvi, B.; Wieczorek, R.; Latajka, Z.; Alikhani, M. E.; Dkhissi, A.; Bouteiller, Y. *J. Chem. Phys.* **1999**, *111*, 6671.
(57) Simon, S.; Bertran, J.; Sodupe, M. *J. Phys. Chem. A* **2001**, *105*, 4359.

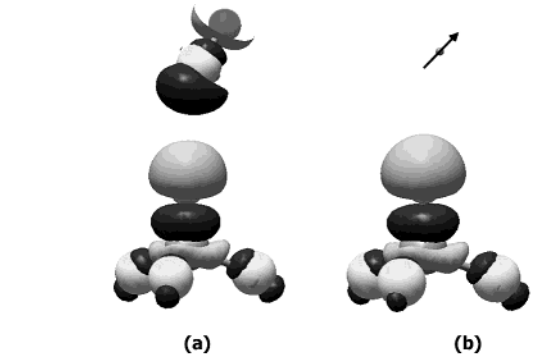

Figure 3. Electron density difference map for (a) $F_3C-H\cdots FH$, (b) $F_3C-H\cdots$dipole.

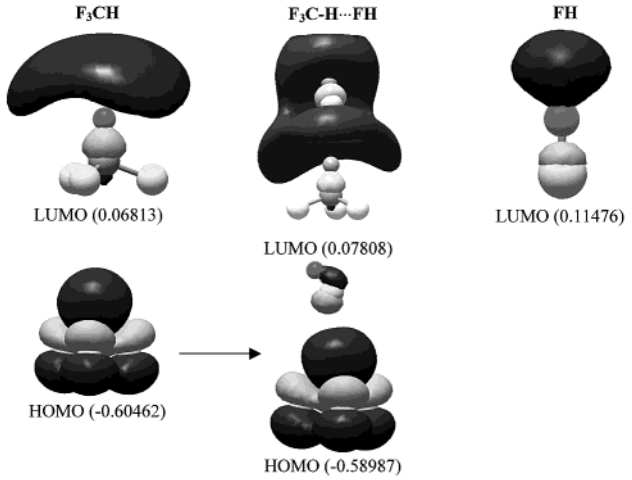

Figure 4. Molecular orbitals for $F_3C-H\cdots FH$.

systems, the net charge transfer is always small. When F_3CH is complexed with a hydrogen acceptor, the F's in F_3CH are more negative, the C in F_3CH is less positive, and the H is more positive than in the monomer. The data show no obvious relationship between the extent of the CH bond blue-shift and the amount of the charge transferred because all of the proton donors in these H-bonded systems tend to lose charge. It must be concluded that the total amount of charge transfer is not a significant contributor to the blue-shift. The change in charges of the atoms in the proton donor comes primarily from the charge redistribution within F_3CH rather than from charge transfer.

What causes this charge redistribution? Electron density difference maps give a more detailed description of the changes in the charge distribution than does NBO or Mulliken population analyses. Figure 3 shows the electron density difference maps for $F_3C-H\cdots FH$ and $F_3CH\cdots$dipole upon complex formation. The dipole is constructed by replacing FH in $F_3C-H\cdots FH$ with two point charges of ± 0.47 (calculated according to CHelpG scheme[58]). The electron density difference plot of the actual blue-shifted system is nearly identical to the one due solely to the electrostatic effect of a dipole. The isodensity value shown in the figure is 0.0005 e/bohr^3. When the isodensity value is increased to 0.001, no surfaces are seen in the electron density difference plot, indicating that the amount of charge redistributed must be less than 0.001 e/bohr^3. The electron density difference of the proton donor in these two systems is in agreement to better than 5×10^{-5}, so it is safe to conclude that the charge redistribution seen in F_3CH is caused by interaction with the

(58) Breneman, C. M.; Wiberg, K. B. *J. Comput. Chem.* **1990**, *11*, 361.

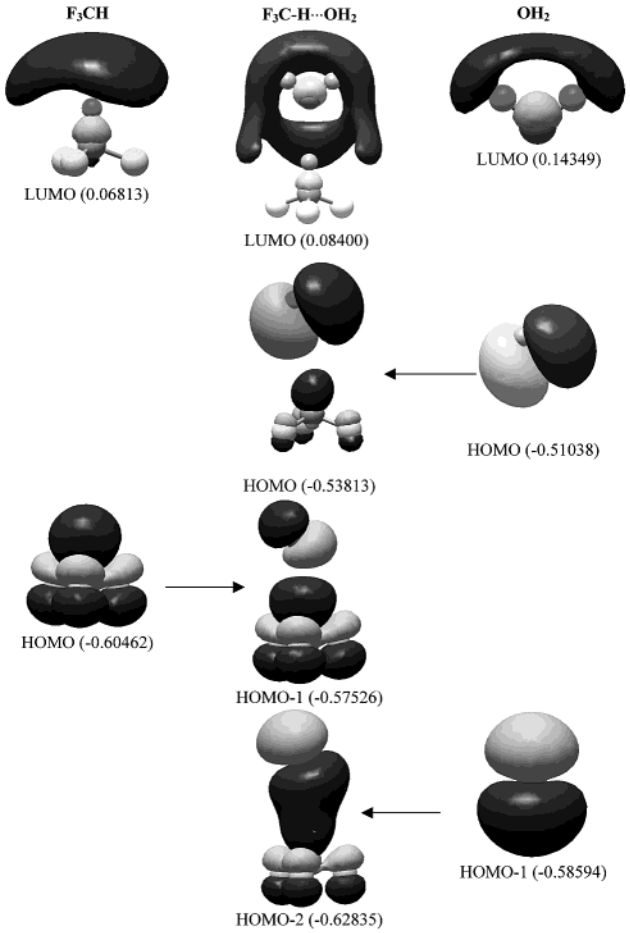

Figure 5. Molecular orbitals for $F_3C-H\cdots OH_2$.

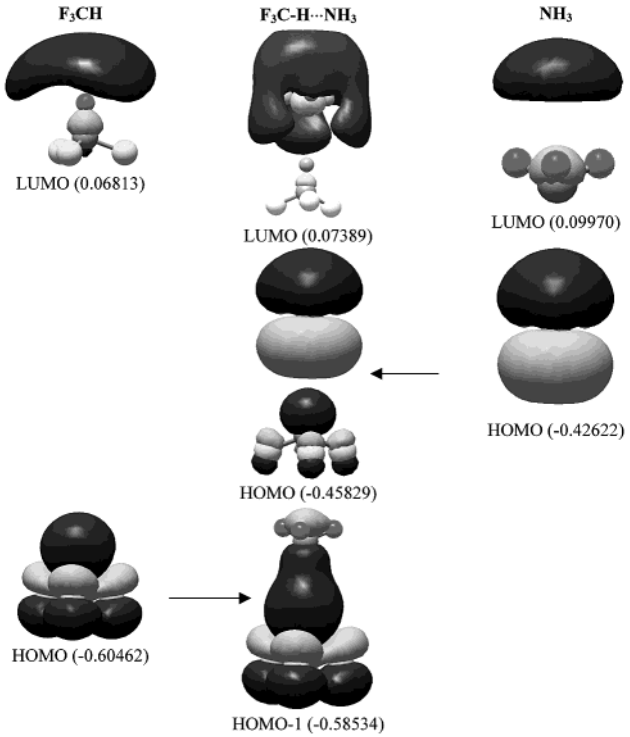

Figure 6. Molecular orbitals for $F_3C-H\cdots NH_3$.

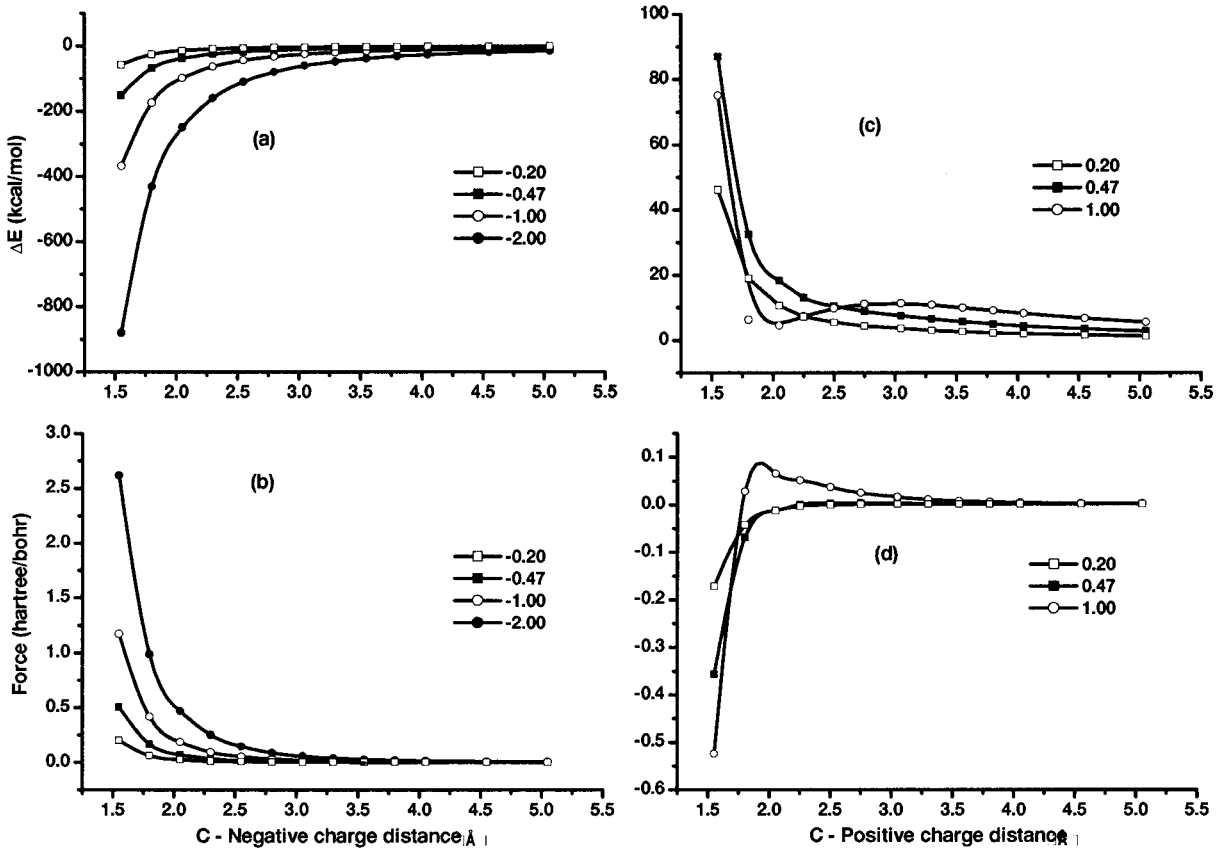

Figure 7. (a) Interaction energy as a function of the distance between carbon and a negative charge; (b) force on C−H bond as a function of the distance between carbon and a negative charge; (c) interaction energy as a function of the distance between carbon and a positive charge; (d) force on C−H bond as a function of the distance between carbon and a positive charge.

dipole of the hydrogen acceptor. Because nearly all of the charge redistribution in F_3CH caused by HF can be modeled with a dipole, the influence of HF on the electron density of F_3CH is predominantly electrostatic in nature.

Because the charge redistribution is small and due to electrostatics, one needs to test whether this is the cause of the blue-shift. To determine if the C−H and C−F bonds would shorten or lengthen in the presence of the dipole, it is sufficient to calculate the forces on the C−H and C−F bonds. Calculation shows that although the dipole moment of the proton acceptor induces a charge redistribution within the proton acceptor, it leads to a positive force (0.003 hartree/bohr) and a lengthening of the C−H bond. The C−F bonds also tend to lengthen upon the interaction with the dipole. By comparison, the forces on the C−H and C−F bonds in the equilibrium $F_3C-H\cdots FH$ system are zero (note these two system are structurally the same). Thus, it is safe to say that the charge redistribution is not the origin of the blue-shift.

E. Orbital Interaction. In Figures 4−6, we show the energies and shapes of the highest occupied and the lowest unoccupied molecular orbital of the $F_3C-H\cdots FH$, $F_3C-H\cdots OH_2$, and $F_3C-H\cdots NH_3$ complexes. The LUMO for each complex is mainly the C−H antibonding orbital mixed with a Y−H antibonding orbital coming from the LUMO of the corresponding proton acceptor. On the other hand, the origins of the HOMOs of the three complexes are quite different. The HOMO of $F_3C-H\cdots FH$ comes mostly from the HOMO of F_3CH (C−H bonding minus F lone pairs), mixed with a minor contribution from a HF σ lone pair. The HOMO-1 to HOMO-5 of $F_3C-H\cdots FH$ are mixtures of various combinations of F lone pairs. In $F_3C-H\cdots OH_2$, the HOMO to HOMO-2 are mixtures of C−H bonding HOMO of F_3CH and lone pairs of H_2O, whereas HOMO-3 to HOMO-5 are purely F lone pairs of the proton donor. For $F_3C-H\cdots NH_3$, HOMO and HOMO-1 are mixtures of the HOMO of F_3CH and the lone pair of NH_3. The N−H bonding orbitals and F lone pairs are also involved in lower lying orbitals.

The charge transfer can be understood in a frontier orbital picture in terms of mixing of the LUMO in one monomer and the HOMO in the other monomer; likewise, electron density redistribution within a monomer is the result of HOMO−LUMO mixing within one monomer. In the simplest approach, this also leads to an increase in the orbital energy of the LUMO and a decrease for the HOMO. If there is mixing of the HOMO of the hydrogen donor (CH bonding orbital) with the LUMO of either the hydrogen acceptor or the hydrogen donor, electron density is lost from the CH bond region accompanied with the elongation of the bond, which is obviously not the origin of the CH bond contraction. Alternatively, mixing of the lone pair (HOMO) of the proton acceptor with the CH antibonding orbital (LUMO) of the proton donor also leads to bond elongation. NBO analysis indicates that this is the dominant interaction. Thus, it is evident that HOMO−LUMO interactions cannot contribute to the shortening of the CH bonds and the blue-shift. However, as can be seen from the figures, the three blue-shifted systems considered involve strong HOMO−HOMO interaction. Moreover, the orbital energies of all of the CH bonds increase upon H-bond formation, as a result of occupied−occupied orbital interaction (i.e., Pauli repulsion).

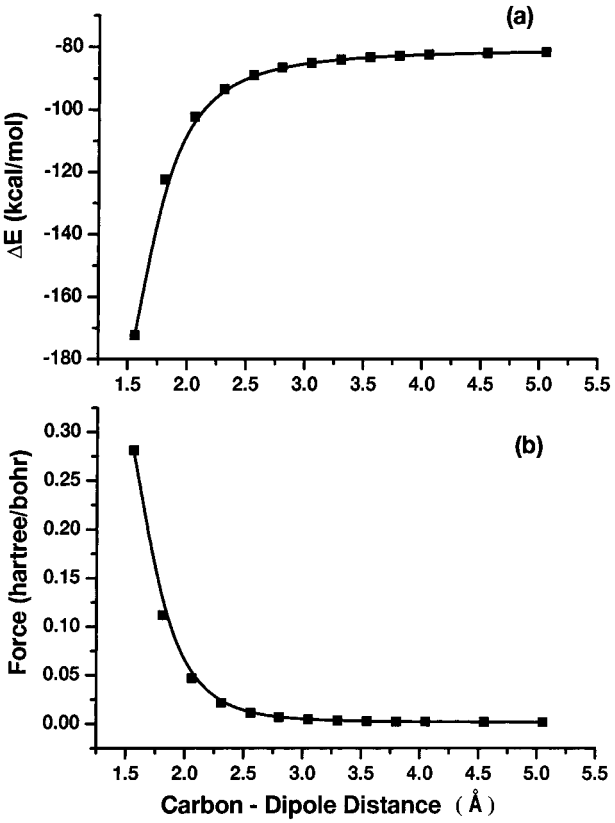

Figure 8. (a) Interaction energy as a function of the distance between carbon and the negative charge of the dipole; (b) force on C−H bond as a function of the distance between carbon and the negative charge of the dipole.

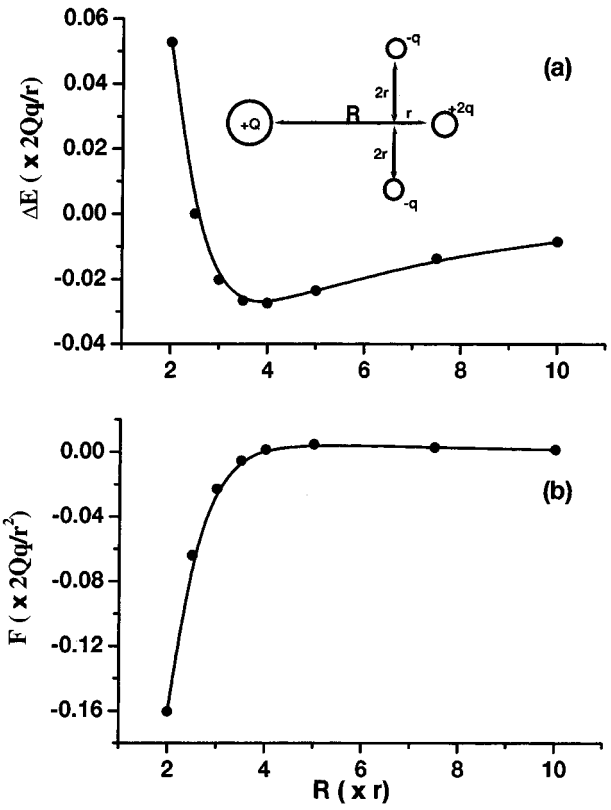

Figure 9. A simple multipole model: (a) Interaction energy as a function of the distance between carbon and the negative charge of the multipole; (b) force on C−H bond as a function of the distance between carbon and the negative charge of the multipole.

F. Electrostatic Interactions. The discussions above indicate that neither charge transfer nor orbital interaction can provide sufficient explanation for the bond contraction and blue-shift in the vibrational frequency. Thus, we need to explore electrostatic interactions. Dykstra et al. have obtained very good agreement with experiment for red-shifted X−H stretching modes in hydrogen-bonded systems by considering only the electrostatic interactions and polarizabilities of the monomers.[9,45−47] In an even simpler model, the interaction of a proton donor with a negative charge was used several decades ago as a conceptual framework for describing hydrogen bonds. In the spirit of this model, a negative point charge was put on the C−H axis at various distances from the carbon of F_3CH. As anticipated, the energy of the system is lowered as the negative charge approaches the CH bond (Figure 7a). The effect of the charge on the CH bond length can be judged easily from the force on the bond (positive force indicates bond elongation). Figure 7b shows that the force is always positive regardless of the distance or the magnitude of the negative charge. An external negative charge elongates the C−H bond, in agreement with previous calculations based on the pure electrostatic interaction model.[10,59,60] Hence, the electrostatic force of a negative point charge cannot induce a blue-shift.

By contrast, a positive charge on the C−H axis produces a repulsive potential energy curve (Figure 7c). At long distances, it attracts the electrons in the C−H bond resulting in a positive force leading to bond elongation. At short distances, the force on the CH bond becomes negative because of repulsion between the positive charge and the nucleus of the hydrogen (Figure 7d). This indicates that the CH bond will contract and its vibrational frequency will be blue-shifted. Nevertheless, it should be noted the F_3CH−positive charge interaction is a not an appropriate model for the hydrogen bond, simply because such an interaction is repulsive in nature.

The interaction between F_3CH and a dipole is a better model of the electrostatic contributions (Figure 8). The dipole is constructed with two point charges of ±0.47 separated by 0.9810 Å so that the dipole moment is equal to HF in F_3C−H···FH. The result is basically the same as that of a single negative charge. The C−H bond elongates as the dipole approaches, and the interaction between F_3CH and the dipole is attractive in nature. This again supports our previous conclusion that it is not simply the electrostatic force field of a dipole that induces the blue-shift.

In an attempt to combine the attractive interactions of a negative charge and the bond shortening repulsion of a positive charge, we can construct a simple multipole model of hydrogen bonding. The model contains two negative charges and one positive charge to represent the proton acceptor as shown in Figure 9. At long range, the dipole interaction dominates, the potential is attractive, and the C−H bond elongates slightly. At short range, the potential is repulsive because of the positive charge, and the C−H bond is compressed. At the minimum in the potential, the bond shortening effect is already noticeable. This simple model demonstrates that a stabilizing interaction and bond shortening can be achieved by an appropriate balance between attractive and repulsive forces.

(59) Vanderijdt, J. G. C. M. V.; Vanduijneveldt, F. B.; Kanters, J. A.; Williams, D. R. *THEOCHEM J. Mol. Struct.* **1984**, *18*, 351.
(60) Hermansson, K. *J. Chem. Phys.* **1991**, *95*, 3578.

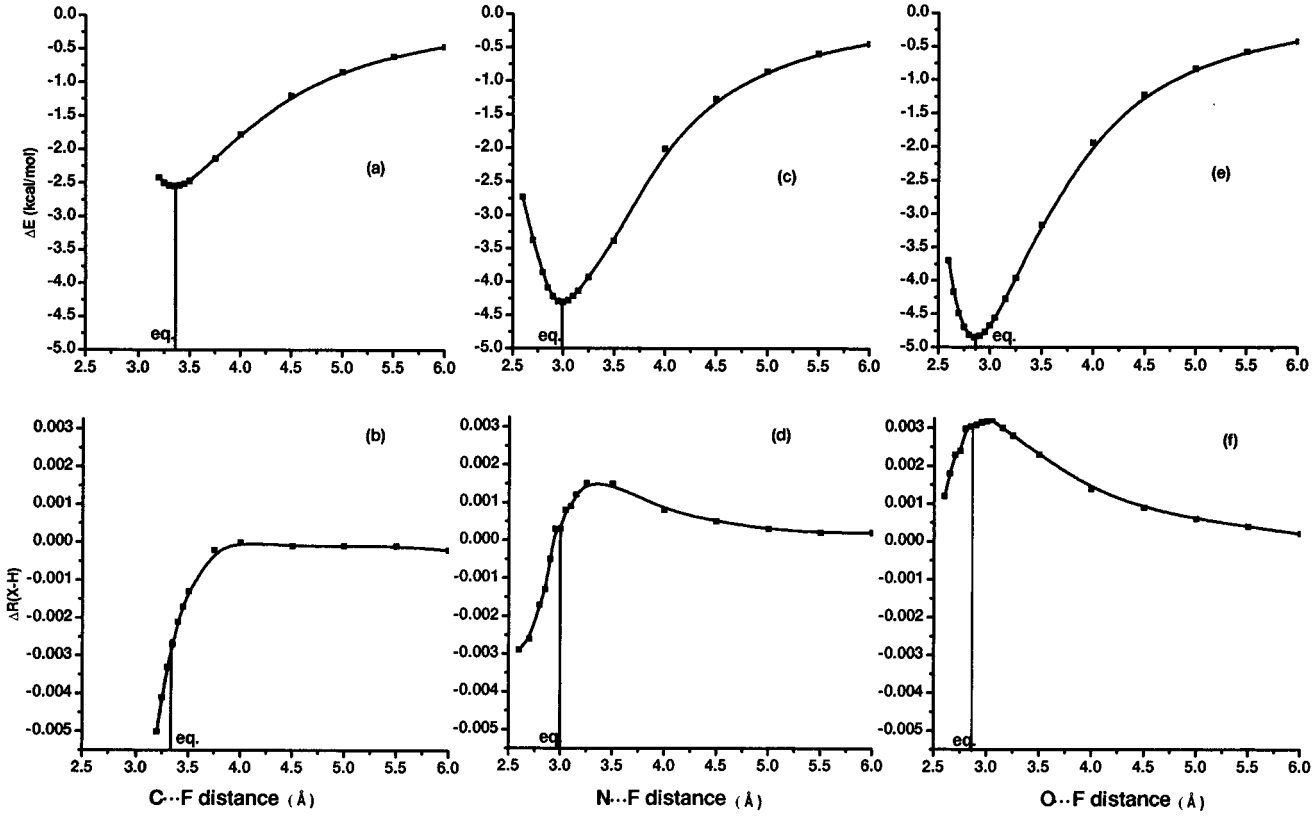

Figure 10. Interaction energy and forces on the C−H bond as a function of the distance between the proton donor and acceptor: (a) and (b) $F_3C-H\cdots FH$, (c) and (d) $F_2N-H\cdots FH$, (e) and (f) $FO-H\cdots FH$ (equilibrium X···F distances indicated by the line labeled "eq").

G. Potential Energy Curves. To determine if the above effect can also be seen in real systems, we studied three complexes: $F_3C-H\cdots FH$, $F_2N-H\cdots FH$, and $FO-H\cdots FH$. The first one has a strong blue-shift, the second has only a small blue-shift, and the third has a strong red-shift. By fixing the C···F, N···F, and O···F distances in $F_3C-H\cdots FH$, $F_2N-H\cdots FH$, and $FO-H\cdots FH$, respectively, and by optimizing the remaining coordinates of the complexes, we obtained curves of the interaction energies and the optimized X−H bond lengths as functions of the X···Y distance (Figure 10).

The potential energy curves are very similar in shape, regardless of whether the hydrogen bond is blue-shifting or red-shifting. At the long distances, the potential energy is proportional to the third power of the reciprocal distance, indicating a dominant dipole−dipole interaction. This is in agreement with Dykstra's finding that the interactions and frequency shifts in regular hydrogen bonds can be explained primarily by electrostatics and polarizability.[9,45−47] For each of the systems, when Y comes closer to X, the X−H length is first elongated, and then compressed. The bond elongation is a result of electrostatic interactions, charge rearrangement, and orbital interactions. For $FO-H\cdots FH$, the charge transfer is much larger than for the other two, indicating much stronger orbital interactions leading to greater bond elongation. The contraction, however, can only be explained as a result of dominant nuclei−nuclei repulsion and electron−electron (Pauli) repulsions, which are significant when the proton donor and acceptor are sufficiently close to each other.

At the minimum in the potential energy curve, there must be a balance between the attractive and repulsion forces. When the proton donor and acceptor approach each other, the X−H bond gradually lengthens; as the short-range repulsive forces come into effect, the bond length goes through a maximum and starts to shorten. By the point that the repulsive (bond compressing) forces balance the attractive forces, the X−H bond is shorter than its maximum elongation. In the absence of orbital interactions, such as in $F_3C-H\cdots FH$, the bond shortening from the repulsion is greater than the elongation from electrostatic effects. In $FO-H\cdots FH$, there are strong orbital interactions (as indicated by the larger charge transfer, see Table 5) that lengthen the O−H bond considerably more than the electrostatic effects alone. The repulsive interactions still shorten the bond, and the O−H bond at the equilibrium geometry is shorter than its maximum elongation. However, this shortening is not enough to compensate the lengthening due to the orbital interactions, and the equilibrium O−H bond length in the complex is longer than that in the monomer.

The difference between blue-shifted and red-shifted hydrogen bonds then becomes simple. For the blue-shifted ones, the bond shortening is greater than bond lengthening when the energy reaches the minimum. On the other hand, for the red-shifted hydrogen bonds, there is an additional bond lengthening due to orbital interactions that is not overcome by the modest bond compression resulting from the repulsive interactions.

A number of observations about blue-shifted hydrogen bonds can be rationalized by this explanation. First, the interactions causing the blue-shift are a balance between electrostatic attraction and steric repulsion (nucleus−nucleus and Pauli repulsion). Therefore, to observe the effect, we do not need a very sophisticated theoretical method; Hartree−Fock is sufficient. The reason that AM1, PM3, and HF/STO-3G fail to predict the phenomenon is probably that they underestimate the

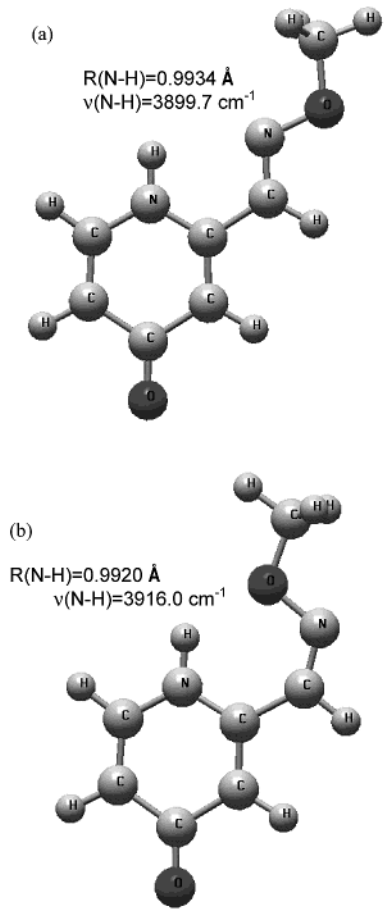

Figure 11. A geometrically constrained hydrogen bonding system (a) not hydrogen bonded, (b) hydrogen bonded, showing a bond shortening and a blue-shift.

repulsion and/or overestimate the orbital interactions. Because the repulsion is not related to hybridization or lone pair electrons of the atoms of the system, it is evident that the blue-shift does not require the central atom of the proton donor to be carbon. The role of fluorination of the proton donors in the blue-shift is primarily to increase the dipole moment of the donor and thus increase the electrostatic interaction with the acceptor. This increased attraction must be balanced by a stronger repulsion, leading to a greater bond shortening and a larger blue-shift.

If the blue-shift is governed by repulsion rather than by the electron-withdrawing fluorines, or the absence of lone pairs on the donor, or dispersion effects, one should be able to construct other examples of blue-shifts. Figure 11 shows the two stable conformers of a reasonable molecule. One is hydrogen bonded; the other is not. The structures were fully optimized at the MP2(FC)/6-311+G(d,p) level of theory. Comparing the N−H bond lengths of the two conformers' complex reveals that the hydrogen bond is compressed (0.9920 for the hydrogen-bonded complex and 0.9934 for the non-hydrogen-bonded complex), leading to a blue-shift of 16 cm^{-1}. However, this is a common N−H···O hydrogen bond that clearly cannot be associated with any electron-withdrawal effect or nonconventional weak interactions. The only possible reason for the blue-shift here is the limited distance between the N and O atoms, so that the proton of the N−H bond must sense significant repulsion from the O atom. Thus, the blue-shifted hydrogen bond here can also be successfully explained as a balance between attractive (electrostatic) and repulsive (steric) forces.

Conclusion

For normal hydrogen bonds, the hydrogen stretching frequency decreases on complexation, but for blue-shifted hydrogen-bonded systems, it increases. This suggested that these phenomena have different physical origins. The present study has shown that both blue-shifted and regular, red-shifted hydrogen bonds are governed by the same interactions.

(a) For $F_3C-H\cdots FH$, calculations were carried out at semiempirical, Hartree−Fock, and post-SCF levels of theory. The blue-shift is reproduced at the Hartree−Fock level with modest basis sets, indicating that electron correlation is not the primary cause of the blue-shift.

(b) Calculations show that $F_3SiH\cdots OH_2$, $F_2NH\cdots FH$, $F_2PH\cdots NH_3$, and $F_2PH\cdots OH_2$ have substantial blue-shifts. Therefore, blue-shifts do not require either a carbon center or the absence of a lone pair on the proton donor.

(c) Interactions between frontier orbitals of the proton donor and acceptor lengthen the X−H bond and lower its vibrational frequency. These interactions are much stronger in regular hydrogen-bonded systems than in blue-shifted complexes. Because these HOMO−LUMO interactions can only lengthen the X−H bond, they cannot be the source of the blue-shift.

(d) The charge redistribution of F_3CH on hydrogen bonding with HF can be reproduced very well by replacing HF with a simple dipole. This indicates that the interactions are predominantly electrostatic.

(e) For complexes involving F_3CH, replacing the proton acceptor with a negative charge yields an attractive interaction but elongates the F_3C-H bond. A positive charge gives a repulsive potential but shortens the bond. Thus, pure electrostatic interactions cannot yield both an attractive interaction and a blue-shift.

(f) At the equilibrium geometry of a complex, the attractive interactions must be balanced by repulsive forces. Electrostatic forces provide the dominant attractive interactions. Pauli repulsion (steric interactions) between two fragments provides the balancing repulsive force. This repulsion shortens the bond and leads to the observed blue-shift in the vibrational frequency.

The balance between attractive and repulsive interactions is present in regular (red-shifted) hydrogen bonds as well as blue-shifted hydrogen bonds. However, in regular hydrogen bonds, strong orbital interactions cause significant bond elongation, overwhelming the shortening caused by the repulsive forces. Thus, the same interactions underlie both red-shifted and blue-shifted hydrogen bonds; the difference is only in the proportion of each.

Acknowledgment. We gratefully acknowledge financial support from the National Science Foundation (CHE 9874005 and CISE 9977815) and a grant from computing resources from NCSA (grant no. CHE980042N).

Supporting Information Available: Cartesian coordinates and total energies for the optimized structures in Table 2 (PDF). This material is available free of charge via the Internet at http://pubs.acs.org.

JA020213J